REAL & REACTIVE POWER LOSS MINIMIZATION IN POWER SYSTEM BY OPTIMIZING SIZE AND LOCATION OF TCSC & SVC USING GREY WOLF OPTIMISATION

[1]Anubha Gautam , [1]P R Sharma, [2]Yogendra Kumar
[1]YMCAUST, Faridabad, [2]MANIT, Bhopal

ABSTRACT–The use of heuristic methods is one of the main advances in research in general since these techniques are capable of adapting themselves to problems for which it is almost impossible to obtain a suitable mathematical model. On the other hand, unlike traditional optimization algorithms, these methods have the ability to incorporate information that is experienced from a particular problem. However, its use in the context of power systems is still in its initial stage, and in this work an application has been presented for the solution of a problem related to the dynamic behaviour of the electrical networks.

An effective way of solving the problem of line loss in electrical power systems is through the injection of reactive power at strategic points in the network. We present a brief description of the problem and the most appropriate measures for its solution, as well as some basic concepts about the reactive power flow in transmission lines. It is concluded that an effective way of attacking the problem is by means of FACTS devicesand particularly with the inclusion of the Static VAR Compensator (SVC) and the Thyristor Controlled Series Compensator (TCSC). Because these devices have convenient features for line loss control,voltage control, in addition to being flexible and allow to incorporate tasks such as damping power oscillations.

In the proposed work the optimal sizing and locationof SVC and TCSC is obtainedusing Grey Wolf Optimization (GWO)technique,having an end goalof loss minimization. The proposed GWO based method validates using IEEE-30 and IEEE-57 bus systems.Here, the Line losses have been efficiently reduced in both these systems during normal load and overloading conditions with the applications of FACTS devices along with GWO.

***KEYWORDS* –EPS, FACTS , GWO, SVC, TCSC.**

I. INTRODUCTION

Power engineering can be considered as one of the oldest and most traditional of all areas of electrical engineering, and we also consider aspects such as: i) the use of modern technology within the operation and planning of systems power; ii) the current structure of the electrical industry facilities, it can be concluded that it is an essential part of the development of electrical engineering. The application of optimization methods is one of the technical improvement tools that has impacted the area in the last twenty years. These methods are very powerful and practical as they are able to ensure a better electrical and economic performance of the electrical power system (EPS).

To analyse the optimization problem, there are many controllable parameters are of interest. There are many objective functions and restrictions that must be satisfied for an economical and reliable operation [1] [2].

The contribution of optimization methods to EPS can be considered to be of great value in economic terms,because hundreds of millions of rupees are saved each year in their operation and planning [3]. In addition, other benefits can be considered in terms of reliability and safety of the electricity network.

In the mid-1960s, the first concepts and optimization algorithms were presented for energy dispatch, resource allocation and EPS planning, mathematically formalizing decision-making, considering a variety of system objectives subject to technical and non-technical constraints [4]. The result was an extraordinary increase in research activities aimed at an optimal implementation of these experiences (optimal power flows). Consequently, there is a great advance in research in the application of optimization methods within power engineering, involving problems related to those systems.

The problem of economic dispatch as a function of time incorporating system constraints is typically solved using optimal power flows (OPF), which is an extension of economic dispatch that includes optimum settings of tap changers under load, active and reactive generation powers, phase changers and some other control device. Other applications extend network optimization work including reactive planning, network expansion, and transferability availability.

It is true that these optimization methods provide great benefits in the electrical industry as they have a great practical application and are very reliable. This is why, in this work we present one of those numerous applications that can be made with the optimization methods.

Generally the EPSis a very complex and non-linear system with dynamics and nonlinearities that cannot be modelled in precise mathematical terms. To implement a controller, it is necessary todecrease the order of the nonlinear model and linearize the equations by considering small deviations around an operating condition. The design of the controller parameters remains fixed.Therefore, the performance of the controllers is affected when there are changes in the operating points.

Recently, many modern optimization techniques have been developed such as Particle Swarm Optimization, Genetic Algorithms and Fuzzy Logic Systems [5], [6], [7], [8], [9], [10], [11], [12]. The applications of these techniques for some problems in EPShave delivered promising results. However, the application of them is still in its initial stage and only recently have begun to receive great attention from researchers.

Modern techniques have a high cost / performance ratio. The aspects described in the previous paragraphs show that the theoretical reasons emphasize generality and precision of the intelligent optimization techniques, while the practical reasons emphasize its applicability and implementation in problems of daily life.

II. GENERAL ASPECTS OF CONTROL IN A POWER SYSTEM

The EPSis generally deliberated so that certain variables can be modified by means of particular device. The control action is achieved by coordinating all the control devices that are connectedto the system. The generalized end goal of the control system can be stated as follows:

- Protection of important parts of the equipment and the integrity of the system.
- Continuity of service with high quality.
- Safe operation of the system.
- Acceptable economic and environmental operation of the system.
- Control in emergency state.
- Restore control in the shortest possible time.

Flexible AC Transmission Systems

FACTS devices are a part of the power electronics insurgency that have been accomplished in a broad segment of electrical engineering. This variety of powerful semiconductors devices provide the possibility of working together on a concept of innovative circuits that improve the characteristics of electric power [13-14].

FACTS technology opens new opportunities to control power and improve the utilization of installed capacity in the transmission network. The use of FACTS devices allows the control corresponding to the flow of power through certain lines, to increase the power transmission capacity under normal operation and system contingency conditions.

The goal of FACTS devices to increase power transmission capacity implies that a given transmission line may be able to operate near its thermal limits, allowing a greater amount of current to flow through its series impedance. At the same time, it must maintain the stability of the system by means of an appropriate real-time control of the power flow during and after a system failure [14].

However, once a large number of these devices are integrated into the system, global coordination and control to provide maximum benefits to the system and prevent undesirable interactions with the different objectives and configurations of the system, covering conditions of normal operation and contingency, present a new technology little explored. This technology must develop appropriate system control and optimization strategies, adequate communication systems and convenient security protocols. The realization of such optimized control of the system can be considered as the third target of the FACTS devices.

III. REACTIVE POWER COMPENSATION

Voltage and reactive power control is one of the areas of greatest attention in the development and operation of an EPS. The importance of the V-Q control comes basically from the need to satisfy the quality requirements in the electric power supply. In addition, an adequate control of reactive power and voltage permits to achieveessentialadvantages in the manoeuvre of the EPSfor example the voltage gradientsreduction, a more effective utilization of the transmission capabilities and in the escalationof the stability limits [15, 16]. The purpose of voltage control is to adjust all nodal voltages within an operating band. This makes the solution of the problem more complex, compared to the frequency control, since there is a multivariate problem. It is convenient to remember that in steady state there is a unique frequency value in the system, whereas all the nodal voltages may be different.

Basic Concepts of Reactive Power Flow

A fundamental aspect of the compensation and control of reactive power is its balance. The shunt capacitance of the transmission line yields reactive power proportional to the square of the voltage. Since the voltage must be kept within ± 5% of the rated voltage, the output or consumption of reactive power is relatively constant. The series inductance of the transmission line consumes reactive power proportional to the square of the current. Since the current varies from the duration of maximum demand to the duration of minimum demand, the reactive power consumption is also modified by the transmission line. Therefore, the net reactive power flux of the transmission line changes with the charge cycle. Figure 1 shows the model for transmission line, where B is the derivation susceptance.

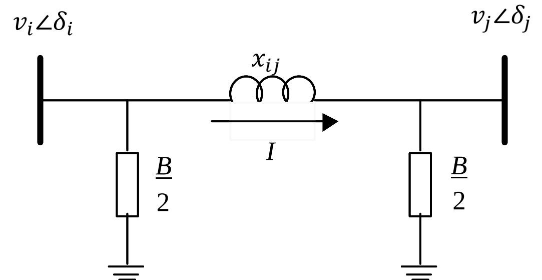

Figure 1: π model of a transmission line

Production of the transmission line = v^2B (relatively constant)

Power consumption of the transmission line = I^2x_{ij} (variable)

As the ratio x/r increases (high-voltage transmission systems where r is the resistance of the transmission line and x its reactance) and the power factor is modified, the effect of the reactive current is greater on the voltage change. This follows from Eq. (1) when analysing the phasor diagram of Fig. 2 [17], where $\Delta v = v_i - v_j$.

$$\Delta v = \frac{P}{v_j} r + \frac{Q}{v_j} x \tag{1}$$

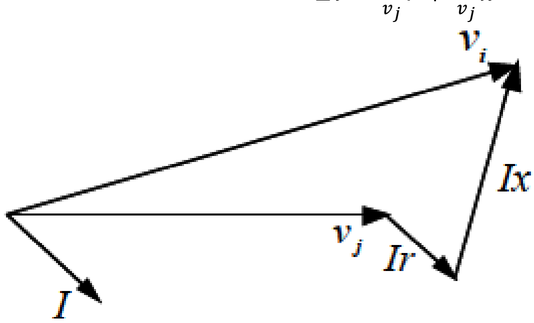

Figure 2: Phasor diagram with delayed power factor

For small angular differences, the reactive power tends to circulate from the highest voltage node to the lowest voltage node, this is determined by the reactive power flow equation (2), for the transmission line shown in Fig. 3.

$$Q_{ij} = \frac{v_i}{x_{ij}} \left(v_i - v_j \cos \delta \right) \tag{2}$$

Where, $\delta = \delta_i - \delta_j$

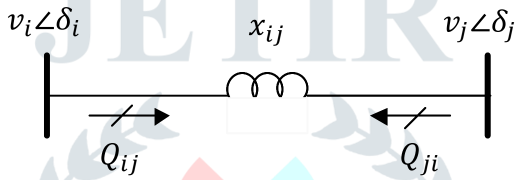

Figure 3: Reactive flow in a transmission line

The losses in the transmission line can be calculated by means of the following expression:

$$Q_p = Q_{ij} + Q_{ji} \tag{3}$$

Substituting the equations of Q_{ij} and Q_{ji}

$$Q_p = \frac{v_i^2}{x_{ij}} + \frac{v_j^2}{x_{ij}} - \frac{2 v_i v_j}{x_{ij}} \cos \delta \tag{4}$$

The reactive losses in equation (4) roughly depend on the voltage difference squared. From the analysis of the equations of reactive flowin a transmission line can be summarized the following fundamental points:

- The reactive flow produces a voltage drop that depends on the reactance of the transmission element.
- Voltage difference increases the reactive power consumption at the reactive element .
- Reactive losses have a non-linear behaviour, with increasing changes having a greater voltage difference.
- The distribution of reactive flows at the ends of the line depends on the charging current and the consumption of reactants at the reactance of the transmission line.

In an EPS, the controlled voltage nodes act the reactive power compensators supplying the necessary reactive, according to the variations of the demand, in such a way to maintain the specified voltage. The result of modifying the voltage generation is a change in the reactive power. Therefore, there is a reactive power exchange between generators, and as a result the voltage profile of the system is altered. The effectiveness of the change depends on reducing the reactive flow in the paths of higher impedance.

According to the concepts presented, it can be concluded that the basic problem to avoid degradation of the voltage profile is to eliminate or reduce the reactive power flow in the system over long distances. Because this involves: greater voltage drops, complication in the control of the same and greater losses resulting from higher currents. Therefore, it implies higher costs of operation and unnecessary use of the thermal capacity of mainly transforming and conducting equipment. It is important to note that in steady state the controls keep the voltage of the controlled node at a specified value. Naturally, there is a tendency to supply the reactive power essential by the load across the lines with less impedance. Equation (5) shows that the ratio of reactive flows depends on the reactances of the branches, Fig. 4 [17].

$$\frac{Q_{ij}}{Q_{kj}} = \frac{x_{kj}}{x_{ij}} \tag{5}$$

Where it is considered that the voltages v_i

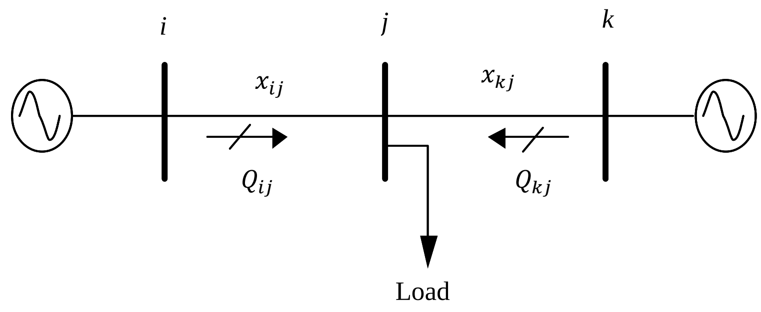

Figure 4: Electrical power system (EPS) of 2 machines

The need for controllable sources of reactive power can be summarized fundamentally in three essential points.

1. Check the voltage at nominal values: When sudden changes in load or topology occur, it may be necessary to correct the voltage in a few cycles. For other voltage variations the correction can be made in seconds. Failure to correct voltage deviations, even if temporary, can result in damage to user equipment.
2. Adjust the voltage profile on the network: In order to avoid the circulation of reactive power and thereby reduce energy losses by making better use of the transmission and transformation equipment capacity.
3. Maintain the timing of the generators: Voltage control through controllable sources of reactive power has stabilizing effects on the EPS, in the presence of disturbances that cause the rotors to change their relative positions. Reactive sources can enhance both small signal stability and transient stability.

That is, the task of voltage control at transmission levels is shared by different control means and operating techniques. The control can be carried out in a discrete way by means of passive compensation equipment in shunt, for example, reactors and capacitors equipped with mechanical switches; changes in transformer leads; with operation manoeuvres, such as opening and closing transmission lines. Another alternative is by means of capacitive series compensation. However, in a continuous way, the voltage control can be carried out basically by the Automatic Voltage Regulators (AVR) of the synchronous machines, Synchronous Capacitors (SC) and by the installation of devices based on electronic power such as SVC and TCSC, which are installed at strategic points in the transmission network [13-14].

In planning to incorporate reactive power compensation devices into an EPS, the following points should be considered and analysed: main device application, sizing, type and location. Responses to the above are not obvious or general. It is necessary to focus them to the particular EPS through complete studies considering different operating conditions. The analysis should include: fault studies, power flow studies, transient and small signal stability studies, transient studies and harmonic studies.

It is difficult to define an appropriate reactive compensation program to control the voltage levels of a system with long transmission lines. One of the first problems is to decide to use derivation or series compensation, or in what quantity each of them should be used [18]. There are some differences in the performance of derivation and series compensation schemes that must be recognized and studied, such as the dynamic performance and transient stability that affect the reliability of these compensating systems. Other differences include the risky sub-synchronous resonance with series capacitors, and harmonic problems associated with power electronics based devices. These factors, as well as the performance of voltage control, are taken into account in EPSplanning and operation studies.

One way of evaluating the most suitable place for the installation of voltage control devices is by means of sensitivity coefficients [19] since these are very useful indicators in the operation of the EPS. Having a large or small coefficient gives a quantitative idea of the expected change in the variables of interest. The sensitivity coefficients should be evaluated for different operating conditions, so that indexes that adequately reflect the expected behaviour are always available [20, 21].

Among the most important applications of these coefficients we can mention:

- Evaluate the change in nodal voltage when connecting a capacitor or reactor to the system.
- Determine changes in the range of reactivein generators by having the connection or disconnection of a reactive element.
- Quantify the influence areas of generators by modifying the generation voltage.
- Evaluate the effectiveness of a tap change to control the voltage of a load node.
- Determine the reactive power losses as a result of a tap change in a transformer.
- Calculate the change in reactive losses as a result of a change in reactive injection.

IV. Static VAR Compensator (SVC)

Static VAR compensators are generally composed of capacitor banks and / or reactors, i.e. passive elements. With the use of power electronics and suitable control strategies an extremely fast response (1 cycle) is achieved to connect shunt elements. The connection / disconnection of capacitors is done discreetly by the control of thyristors in the driving periods. The reactor connection is carried out in a controlled manner by varying the firing angle of the thyristors, thus achieving continuous control of the reactor current.

In the transmission systems the proper characteristics of voltage control and reactive power with SVCs are usually obtained based on closed-loop control strategies [22, 23]. Making the distinction of the different hierarchies of operation, the control scheme of the SVC consists of a primary voltage regulation loop and in some compensation schemes, a secondary superimposed loop of reactive power control [24, 25]. From the analysis of the control loop, the quasi-static operational or steady-state characteristics of the EPS are determined. Also, the analysis of the closed loop transfer function establishes the stability characteristics of the control loop and its dependence on the state of operation of the EPS. The control logic is determined by a voltage controller whose simplest form is of proportional characteristic, which translates the error signal into a change signal in the compensator susceptance [23], where I_{SVC} is the current flowing from the terminals of the SVC to the system, B_{SVC} is the SVC equivalent susceptance, v_t is the voltage at the EPS terminals, V_v is the signal proportional to the magnitude of the voltage at terminals, $G_m(s)$ is the transfer function of the measuring device, $G_r(s)$ is the transfer function of the voltage controller, and $G_y(s)$ is the transfer function of the trigger control scheme in thyristors.

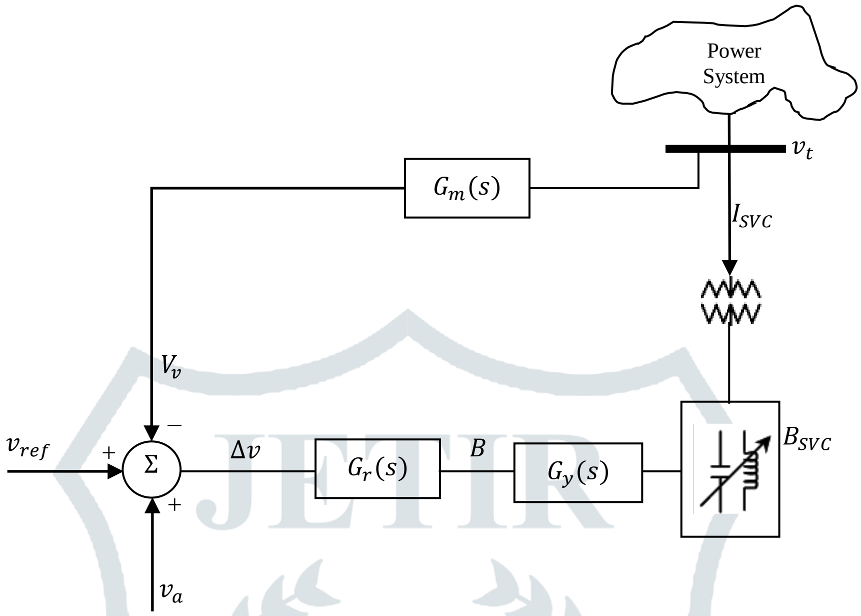

Figure 5: Control scheme of an SVC using voltage feedback

From the point of view of operation, the characteristic of interest is the relation between the voltage in terminals and the current provided by the compensator, that is:

$$I_{SVC} = B_{SVC} v_t \tag{6}$$

The graphical representation of equation (6) is known as the steady-state control characteristic curve of a static compensator. Its determination is important since it defines the operation of the SVC within the linear range of control. The operating characteristic curve of the compensator is shown in Figure 6 and is a function of the two steady-state control parameters: the reference voltage v_{ref}, and the adjustable slope of the operating curve. k_a is the gain of the controller; the voltage is regulated as per this characteristic slope [26].

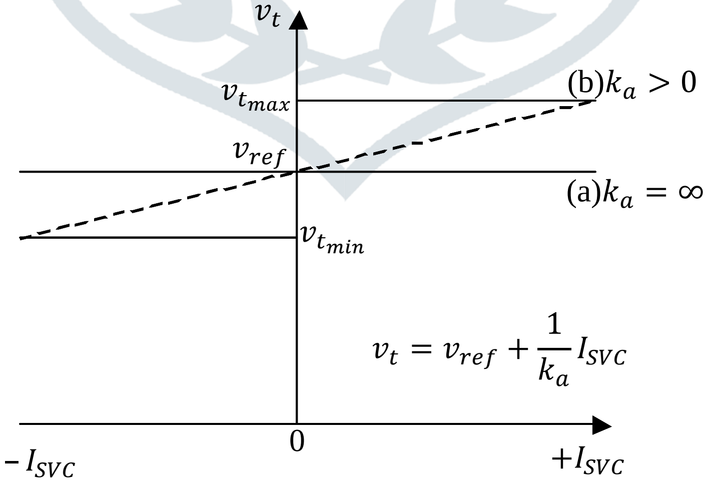

Figure 6: Operating characteristic of an SVC

Two forms of voltage control can be performed according to the slope selection:

1. Rigid (flat) voltage control. In this scheme an infinite voltage regulator gain is required, implying a constant voltage at the compensator terminals for any operating condition.
2. Polarized voltage control. In this scheme the gain of the voltage regulator has a positive finite value, allowing some variation in the magnitude of the voltage around the reference value.

For large gain of the voltage controller, small slopes of the characteristic curve are obtained, thus increasing the speed of response of the compensator. A similar effect is achieved by decreasing the value of the controller's time constants. The second factor influencing the SVC response is the short-circuit capability of the EPS. It is important to mention that for voltage regulation studies the operating characteristic of the EPSis defined by its equivalent of Thevenin seen from the compensated node, where the impedance of the system is considered approximately equal to the short-circuit reactance [23]. The compensator response is very fast for the weakest operating conditions. That is, for a system with a shorter short-circuit capacity. Respectively an increase in the level of short circuit results in a slower response of the compensator. The slope value is determined on the basis of dynamic and steady-state studies of the EPS. Therefore, practically the stability requirements and response time of the control loop, should be determined by appropriate selection of the time constant of the voltage regulator [24, 25].

The characteristic curve consists of three zones or control ranges that are of interest [27, 28, 29]:

1. A linear zone of operation defined by the compensator control scheme. The voltage at the SVC terminals is regulated between its minimum and maximum operating limits $v_{t_{min}}$ and $v_{t_{max}}$, respectively.
2. A low voltage operating area. In this the compensator operates at its minimum control limit, thus losing its capacity as a voltage regulating element. This zone seen from the EPS indicates that the operation of the SVC is determined by the nominal capacity of its capacitive branch, with the voltage in terminals varying between 0 and $v_{t_{min}}$, as per the need of the electrical system.
3. An overvoltage operating area. In this one the compensator operates in its maximum value of control, arising a characteristic of variation of voltage in terminals of the SVC, corresponding to the one of a fixed reactor with a nominal capacity equal to the inductive branch of the SVC.

In analytical form, the voltage regulating characteristic of the compensator in its nominal operating range is expressed by:

$$v_t = v_{ref} + mI_{SVC} \tag{7}$$

Where m is the slope of the characteristic curve and I_{SVC} satisfies the constraints:

$$I_{S_{min}} < I_{SVC} < I_{S_{max}} \tag{8}$$

Where $I_{S_{min}}$ and $I_{S_{max}}$ representthe nominal capacitances of current injection in the capacitive and inductive branches of the compensator respectively.

According to the control of the compensator the operation of the SVC in the area of low voltage corresponds to a fixed capacitor, described by the relation:

$$I_{SVC} = B_{S_{min}} v_t \tag{9}$$

Where $B_{S_{min}}$ represents the nominal capacity of the SVC capacitor branch.

In the overvoltage range the SVC operating characteristic corresponds to that of a fixed reactor of $B_{S_{max}}$ capacity with:

$$I_{SVC} = B_{S_{max}} v_t \tag{10}$$

In general, only the operation of the compensator within its nominal control range represents a desirable voltage regulation characteristic, the other two being considered as degraded modes of operation [23].

The reactive power caused by the SVC, that is the reactive power inserted at bus k, is expressed as:

$$Q_{SVC} = Q_k = -v_t^2 B_{SVC} \tag{11}$$

Now the equation (12) represents the linearized form of the SVC where the equivalent susceptance, B_{SVC} is considered as state variable:

$$\begin{bmatrix} \Delta P_k \\ \Delta Q_k \end{bmatrix}^{(i)} = \begin{bmatrix} 0 & 0 \\ 0 & Q_k \end{bmatrix}^{(i)} \begin{bmatrix} \Delta\theta_k \\ \Delta B_{SVC}/B_{SVC} \end{bmatrix}^{(i)} \tag{12}$$

Towards the end of iteration (i), B_{SVC}varies:

$$B_{SVC}^{(i)} = B_{SVC}^{(i-1)} + \left[\frac{\Delta B_{SVC}}{B_{SVC}}\right]^{(i)} B_{SVC}^{(i-1)} \tag{13}$$

This varyingsusceptance characterizes the overall SVCsusceptance required to sustain the nodal voltagemagnitude at the specific value.

V. Thyristor Controlled Series Compensator (TCSC)

This device is widely used for the control of flow of power in the transmission lines through a series compensation. The function of a TCSC, is to transform the impedance of the line, inserting capacitors or inductances in series with the circuit to modify the power flow. The capacitive compensation is the most used, because it helps to rectify the natural inductive effects of the transmission lines.

The advantage of the TCSC over conventional stabilizers is that these devices with mechanical drives, which over time and use tend to wear out and suffer breakdowns, whereas the TCSC when using static drive devices based on Thyristors do not have this problem due to mechanical stress [30].

For the modeling of a TCSC in a transmission line, the simplified model is taken from the line and in series to the line impedance, a X_{TCSC} variable reactance is placed, representing the inductive or capacitive capacitance that the compensator has over the Line as shown in figure 7.

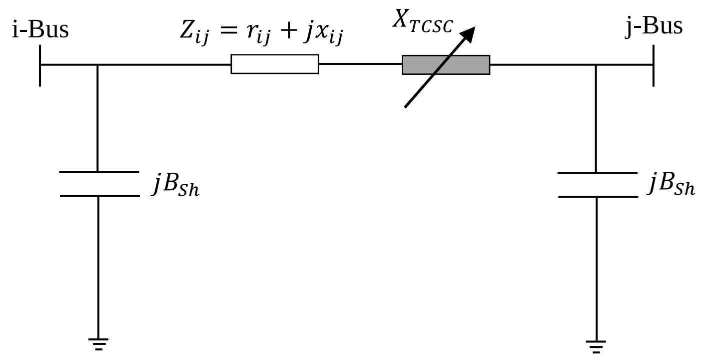

Figure 7: Diagram of a transmission line compensated with a TCSC [31]

TCSC Modeling

During the steady state, the compensator can freely change between reactance values according to its control. To avoid over-compensation of the line, limits are recommended for the reactance oscillation, given by the equation (14).

$$-0.8\, X_L \leq X_{TCSC} \leq 0.2\, X_L p.u. \tag{14}$$

The proposed limit vary among different research works, but a tendency of capacitive factor greater than 50% of reactance of the line and inductive factor less than 25% of the inductance of the line is maintained.

In order to be used in a power flow, the model must be in a line impedance with the built-in transformer reactance, in order to obtain the scheme shown in Figure 8, the reactance variations introduced by the compensator are expressed through the variation equation (14).

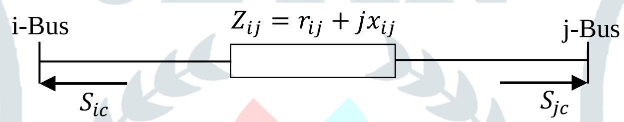

Figure 8: TCSC Power Injection Model [31]

$$\Delta y_{i,j} = y'_{i,j} - y_{i,j} = \left(G'_{i,j} + jB'_{i,j}\right) - \left(G_{i,j} + jB_{i,j}\right) \tag{15}$$

Where

$$G_{i,j} + jB_{i,j} = \frac{1}{Z_{i,j}} \tag{16}$$

$$G_{i,j} = \frac{r_{i,j}}{r_{i,j}^2 + x_{i,j}^2},\ G_{i,j} = \frac{-x_{i,j}}{r_{i,j}^2 + x_{i,j}^2} \tag{17}$$

$$G'_{i,j} = \frac{r_{i,j}}{r_{i,j}^2 + \left(x_{i,j} + x_{TCSC}\right)^2},\ G'_{i,j} = \frac{-\left(x_{i,j} + x_{TCSC}\right)}{r_{i,j}^2 + \left(x_{i,j} + x_{TCSC}\right)^2} \tag{18}$$

In function (15) it is stated that in fact there is a variation of admittances by the presence of the compensator, so that the admittances matrix will also be affected in the mean indicating (19).

$$Y'_{BUS} = Y_{BUS} + \begin{array}{c} \left[\begin{array}{ccccccc} 0 & 0 & 0 & \cdots & 0 & 0 & 0 \\ 0 & \Delta y_{i,j} & 0 & \cdots & 0 & -\Delta y_{i,j} & 0 \\ 0 & 0 & 0 & \cdots & 0 & 0 & 0 \\ \cdots & \cdots & \cdots & \cdots & \cdots & \cdots & \cdots \\ 0 & 0 & 0 & \cdots & 0 & 0 & 0 \\ 0 & -\Delta y_{i,j} & 0 & \cdots & 0 & \Delta y_{i,j} & 0 \\ 0 & 0 & 0 & \cdots & 0 & 0 & 0 \end{array}\right] \\ Col-i \quad \ldots \quad Col-j \end{array} \begin{array}{l} \\ \\ Line-i \\ Line-j \\ \\ \end{array} \tag{19}$$

In terms of power flows between bars, the equations denoting power with the addition of the compensator can be written for active and reactive power flow, applying the admittance variation produced by the compensator series so that they are obtained [32, 33]:

$$P_{ijTCSC} = V_i^2 G'_{i,j} - V_i V_j [G'_{i,j} Cos\left(\delta_{ij}\right) - B'_{i,j} Sin\left(\delta_{ij}\right)] \tag{20}$$

$$Q_{ijTCSC} = -V_i^2\left(B'_{ij} + B_{sh}\right) + V_i V_j [G'_{ij} Sin\left(\delta_{ij}\right) - B'_{ij} Cos\left(\delta_{ij}\right)] \tag{21}$$

VI. PROBLEM FORMULATION

A very large part of the power losses in the electrical networks are attributed to those of distribution. On the whole power carried by the electrical power system, the power losses are estimated at 14%. The level of these losses combined with the deregulation of the electricity marketplace has prompted the distribution companies to give serious consideration to the problem of losses in the EPS in order to increase the power transmission of the latter before thinking of invest in the construction of new lines.

For a given line configuration and given that the demand for active power is incompressible, the reduction of voltage drops and that of power losses can only be achieved by reducing the transit of the reactive component. For this purpose reactive energy compensation is optionali.e. the shunt capacitor..

The optimization of the reactive energy compensation is to be understood as the choice of the capacitor bank capacitances, their locations and even the time they will remain in line if it is an adaptive compensation. Of course, these choices have to be made so that there is the least power loss in line and an improvement in the voltage profile while having a positive economic return. The choices of the objective function are dictated by the concern to take into account both the electrical and economic aspects of the problem.

This paper proposes a system for reduction of power loss using localization and sizing of FACTSdevice. The objective function is modelled as follows:

$$Minimise\ F = \sum_{i=1}^{Nl} Pli + \sum_{i=1}^{Nl} Qli (22)$$

Where *Pli* is active power loss of ith line,*Qli* is the reactive power loss of ith line, *Nl* is the total number of lines.

Subject to the equality constraints:

$$a)\ P_{gi} - P_{di} - P_i(V_i, \delta_i) = 0$$

$$b)\ Q_{gi} - Q_{di} - Q_i(V_i, \delta_i) = 0$$

And inequality constraints:

$$a)\ P_{gi}^{Min} \leq P_{gi} \leq P_{gi}^{Max}$$

$$b)\ Q_{gi}^{Min} \leq Q_{gi} \leq Q_{gi}^{Max}$$

$$c)\ V_{i\,min} \leq V_i \leq V_{i\,max}$$

$$d) - 0.8\, X_L \leq X_{tcsc} \leq 0.2\, X_{tcsc}$$

$$e) - 0.2pu \leq B_{svc} \leq 0.2pu$$

Where Pgi and Qgi are the active and reactive power generated at bus i,.Pdi and Qdi are the active and reactive power at load bus i, Vi is the voltage magnitude at bus i., Xtcsc is the reactance of the TCSC, Bsvc is the suceptance of SVC.

VII. Newton-Raphson Technique for Load Flow Analysis

Let us assume that:

$$S_i = I_i^* V_i \quad (23)$$

$$I_i^* = \sum_{m=1}^{n} Y_{im}{}^* V_m^* \quad (24)$$

$$Y_{im} = \rho_{im} + j\beta_{im} \quad (25)$$

The variation of the active power is less sensitive to the variation of the voltage V. Then again, it is more sensitive to that of phaseδ. On the other hand, the variation of the reactive power is more sensitive to the variation of the voltage V and is less sensitive to that of phase δ. The elements of JACOBIEN J_{PV} are calculated [34] [35]:

$$\frac{\partial P_i}{\partial |V_j|} = |V_i|.|Y_{ij}|.\cos(\theta_{ij} - \delta_i + \delta_j) \quad (26)$$

Where, $\theta_{ij} \approx 90°\ and \delta_i \approx \delta_j$ then $\frac{\partial P_i}{\partial |V_j|} \approx |V_i|.|Y_{ij}|.\cos(90°)$=0.0

Now, we calculate the elements of JACOBIAN $J_{Q\delta}$:

$$\frac{\partial Q_i}{\partial |\delta_j|} = -|V_i|.|V_j|.|Y_{ij}|.\cos(\theta_{ij} - \delta_i + \delta_j) \quad (27)$$

Where, $\theta_{ij} \approx 90°\ and \delta_i \approx \delta_j$ then $\frac{\partial Q_i}{\partial |\delta_j|} \approx -|V_i|.|V_j|.|Y_{ij}|.\cos(90°)$= 0.0

Consequently, the sub-matrices of the JACOBIEN $J_{Q\delta}$ and J_{PV} are null.

$$\begin{bmatrix} \Delta P \\ \Delta Q \end{bmatrix} = \begin{bmatrix} J_{P\gamma} & 0 \\ 0 & J_{QV} \end{bmatrix} . \begin{bmatrix} \Delta\delta \\ \Delta V \end{bmatrix} \Rightarrow \begin{matrix} \Delta P = J_{P\delta}.\Delta\delta = \frac{\partial P}{\partial \delta}.\Delta\delta \\ \Delta Q = J_{QV}.\Delta|V| = \frac{\partial Q}{\partial |V|}.\Delta|V| \end{matrix} \quad (28)$$

The elements of JACOBIEN $J_{P\delta}$are calculated:

$$\frac{\partial P_i}{\partial \delta_i} = ? \quad (29)$$

$$\frac{\partial P_i}{\partial \delta_i} = \sum_{\substack{j= \\ j\neq i}}^{N} |V_i|.|V_j|.|Y_{ij}|.\sin(\theta_{ij} - \delta_i + \delta_j) = -|V_i|^2.|Y_{ii}|.\sin(\theta_{ii}) + \sum_{\substack{j= \\ j\neq i}}^{N} |V_i|.|V_j|.|Y_{ij}|.\sin(\theta_{ij} - \delta_i + \delta_j) \quad (30)$$

Where,

$$\frac{\partial P_i}{\partial \delta_i} = -|V_i|^2.|Y_{ii}|.\sin(\theta_{ii}) - Q_i \quad (31)$$

And

$$Q_i = \sum_{j=1}^{N} |V_i|.|V_j|.|Y_{ij}|.\sin(\theta_{ij} - \delta_i + \delta_j) \tag{32}$$

$|Y_{ii}|.\sin(\theta_{ii}) = B_{ii}$, $B_{ii} \gg Q_I \frac{\partial P_i}{\partial \delta_i} = -|V_i|^2.B_{ii}$ and $|V_i|^2 = |V_i|$ so $\frac{\partial P_i}{\partial \delta_i} = -|V_i|.B_{ii}$

Now we calculate $\frac{\partial P_i}{\partial \delta_j} = ?$

$$\frac{\partial P_i}{\partial \delta_j} = -|V_i|.|V_j|.|Y_{ij}|.\sin(\theta_{ij} - \delta_i + \delta_j) \tag{33}$$

Since $\delta_j - \delta_i \approx 0$, therefore,

$$\frac{\partial P_i}{\partial \delta_j} = -|V_i|.|V_j|.|Y_{ij}|.\sin(\theta_{ij}) \tag{34}$$

Where, $|Y_{ij}|.\sin(\theta_{ij}) = B_{ij}$, $|V_j| \approx 1$

$$\frac{\partial P_i}{\partial \delta_j} = -|V_j|.B_{ij} \tag{35}$$

The elements of Jacobian J_{QV} are calculated:

$$\frac{\partial Q_i}{\partial V_j} = ? \tag{36}$$

$$\frac{\partial Q_i}{\partial |V_i|} = -2.|V_i|.|Y_{ii}|.\sin(\theta_{ii}) - \sum_{\substack{j=1 \\ j\neq i}}^{n} |V_j|.|Y_{ij}|.\sin(\theta_{ij} - \delta_i + \delta_j) \tag{37}$$

$$\frac{\partial Q_i}{\partial |V_i|} = -|V_i|.|Y_{ij}|.\sin(\theta_{ii}) - |V_i|^{-1} \sum_{j=1}^{n} |V_i|.|V_j|.|Y_{ij}|.\sin(\theta_{ij} - \delta_i + \delta_j) \tag{38}$$

$$\frac{\partial Q_i}{\partial |V_i|} = -|V_i|.|Y_{ii}|.\sin(\theta_{ii}) - |V_i|^{-1}.Q_i \tag{39}$$

Where $Q_i = -\sum_{j=1}^{n} |V_i|.|V_j|.|Y_{ij}|.\sin(\theta_{ij} - \delta_i + \delta_j)$

$|Y_{ii}|.\sin(\theta_{ii}) = B_{ii}$, $B_{ii} \gg Q \Longrightarrow \frac{\partial Q_i}{\partial |V_i|} = -|V_i|.B_{ii}$ And $\frac{\partial Q_i}{\partial |V_j|} = ?$

$$\frac{\partial Q_i}{\partial |V_j|} = -|V_i|.|Y_{ii}|.\sin(\theta_{ij} - \delta_i + \delta_j) \tag{40}$$

Since $\delta_j - \delta_i \approx 0$, therefore,

$$\frac{\partial Q_i}{\partial |V_j|} = -|V_i|.|Y_{ii}|.\sin(\theta_{ij}) \tag{41}$$

Where, $|Y_{ii}|.\sin(\theta_{ij}) = \mathrm{B_{ii}}$, $\frac{\partial Q_i}{\partial |V_j|} = -|V_i|.B_{ii}$

The individual power change equations in $J_{P\delta}$ and J_{QV} are:

$$\Delta P_i = \sum_{J=1}^{N} -|V_i|.B_{ij}.\Delta\delta_j \qquad \Longrightarrow \frac{\Delta P_i}{|V_i|} = \sum_{J=1}^{N} -B_{ij}.\Delta\delta_j \tag{41}$$

$$\Delta Q_i = \sum_{J=1}^{N} -|V_i|.B_{ij}.\Delta|V_j| \qquad \Longrightarrow \frac{\Delta Q_i}{|V_i|} = \sum_{J=1}^{N} -B_{ij}.\Delta|V_j| \tag{42}$$

$$\frac{\Delta P}{|V_i|} = -B'.\Delta\delta \qquad \Longrightarrow \Delta\delta = -[B']^{-1}.\frac{\Delta P}{|V_i|} \tag{43}$$

$$\frac{\Delta Q_i}{|V_i|} = -B''.\Delta|V| \qquad \Longrightarrow \Delta|V| = -[B'']^{-1}.\frac{\Delta Q_i}{|V_i|} \tag{44}$$

The fast decoupled method FDL performs the same execution times as that of Newton-Raphson for very small networks. However, it becomes faster for more and the usual tolerances.

VIII. Optimal Location using Grey Wolf Optimization

The location and sizing of FACT device for any specific bus system is optimized by Grey Wolf Optimization (GWO) [36]. The objective function is minimized using the above-mentioned technique.

The GWO algorithm simulates the natural behaviour of a mob of wolves to hunt its prey. Within the wolves' different categories are distinguished as in a more forceful way in the search space. The pseudo-code is presented in GWO Algorithm. At the end of the execution, the best individual is going to be starts with a value of 2 and decrementing along the evaluations until they reach 0. They help the candidate solutions, moving them in the search space. The key to the algorithm is found in the function *updateposition*(..) (See line no.8 of GWO Algorithm) which is defined as [36]:

$$\vec{X}_{li} = \frac{\vec{X}_1 + \vec{X}_2 + \vec{X}_3}{3} \tag{45}$$

Where each $\vec{X}_1$, $\vec{X}_2$ and $\vec{X}_3$ is obtained as follows:

$$\vec{X}_1 = |\vec{x}_\alpha - \vec{A}_\alpha * \vec{D}_\alpha|, \quad \vec{X}_2 = |\vec{x}_\beta - \vec{A}_\beta * \vec{D}_\beta|, \quad \vec{X}_3 = |\vec{x}_\delta - \vec{A}_\delta * \vec{D}_\delta| \tag{46}$$

To determine $\vec{D}_\alpha$, $\vec{D}_\beta$ and $\vec{D}_\delta$, used in equation (46), the following formulas are used:

$$\vec{D}_\alpha = |\vec{C}_1.\vec{X}_\alpha - \vec{X}|, \ \vec{D}_\beta = |\vec{C}_2.\vec{X}_\beta - \vec{X}|, \ \vec{D}_\delta = |\vec{C}_3.\vec{X}_\delta - \vec{X}| \tag{47}$$

GWO Algorithm

1. generate (X) / / Initialize the population of grey wolves
2. initializeParameter (a, A, C);
3. evaluate X (0);
4. select new (Alpha, Beta, Delta, X (0));
5. for e = 1 to EVALMAX to do

```
6.for every Wolf l in Omega do
7.      for i = 0 to DIM do
8.         update Position (l, i); // Update current position
9.      end for
10.     adjust parameters (a, A, c); // adjust the algorithm parameters
11.     evaluate X (e + 1);
12.     select new (Alpha, Beta, Delta, X (e + 1));
13.     e = e + 1;
14.  end for
15. end for
```

IX. RESULTS AND DISCUSSIONS

For validation of proposed technique , GWO has been tested on IEEE 30 bus and IEEE 57 bus system. In this study the location and reactance of the TCSC is obtained using GWO for loss minimization.

Test Case 1 , IEEE-30 Bus Systems :

Table no 1. Comparison of active & reactive power loss for different loading conditions using TCSC at different locations obtained by GWO.

Losses	Loading Condition	Without Device	With TCSC GWO	Location of TCSC (Line no)	Xtcsc
Active Power Losses (MW)	Normal Loading	17.4872	2.7715	5	-0.2615
	110% Loading	21.672	3.1349	8	-0.2624
	125% Loading	28.959	8.8054	9	-0.2288
Reactive Power Losses (MVAR)	Normal Loading	69.2327	17.334	5	-0.2615
	110% Loading	85.1068	21.823	8	-0.2624
	125% Loading	112.65	37.006	9	-0.2288

As shown intable 1,IEEE 30 bus system is the test case ,which is subjected to 110% and 125% overloading. As a result, the total active power demand raises to 311.74 MW (for 110% loading) and 354.25 MW (for 125% loading) from normal loading requirement of 283.4 MW. To reduce the system losses firstly the optimal size and location of TCSC is obtained using GWO.

It can be seen from table 1 that for normal loading conditions GWO finds the line number 9 as optimal location for TCSC which is having an optimal size of -0.2615 pu. As a result of which the active power loss reduces from 17.4872MW to 2.7715 MW,while the reactive power losses are diminished from 69.2327 MVAR to 17.334 MVAR. Similarly active power losses are initially 21.672MW& 28.959MW for 110% overloading & 125% overloading respectively, but after the optimal placement of TCSC in line number 9 these losses are reduced to 3.1349MW & 8.8054MW respectively. Also reactive power losses are reduced to 21.823MVAR and 37.006 MVAR from an initial value of 85.1068 MVAR and 112.65 MVAR respectively for 110% and 125% overloading respectively.

Table no 2. Comparison of active & reactive power loss for different loading conditions using SVC at different locations obtained by GWO

Losses	Loading Condition	Without Device	With SVC GWO	Location of SVC (Bus No.)	Bsvc
Active Power Losses (MW)	Normal Loading	17.4872	16.8727	3	0.2473
	110% Loading	21.672	21.2829	3	0.2478
	125% Loading	28.959	28.426	5	0.247
Reactive Power Losses(MVAR)	Normal Loading	69.2327	67.8167	3	0.2473
	110% Loading	85.1068	84.3898	3	0.2478
	125% Loading	112.65	111.6564	5	0.247

As refer to table 2 , for normal loading conditions the optimal location of SVC as obtained by GWO is bus number 3 and its optimal size is 0.2473 pu. Here the SVC reduces active power losses from 17.4872MW to 16.8727MW .while the reactive power losses are reduced from 69.2327 MVAR to 67.8167MVAR.similarly for 110% and 125% overloading active power losses are reduced from 21.672MW and 28.959 MW to 21.2829 MW and 28.426 MW respectively.Also Optimal placement of SVC is minimizing the reactive power losses from 85.1068MVAR to 84.3898MVAR for 110 % loading while reducing the reactive power losses from 112.65MVAR to 111.6564 MVAR for 125% overloading.

It can be concluded from the above results that TCSC is more effective in reducing the active as well as reactive power losses in normal as well as overloading conditions as compared to SVC. The comparison between the results of TCSC and SVC are shown in the following figures from fig.9-fig.16

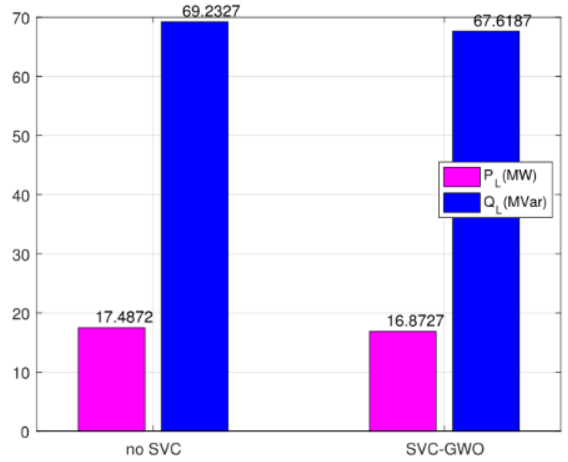

Fig:9 Active and Reactive power loss in Normal Loading using SVC

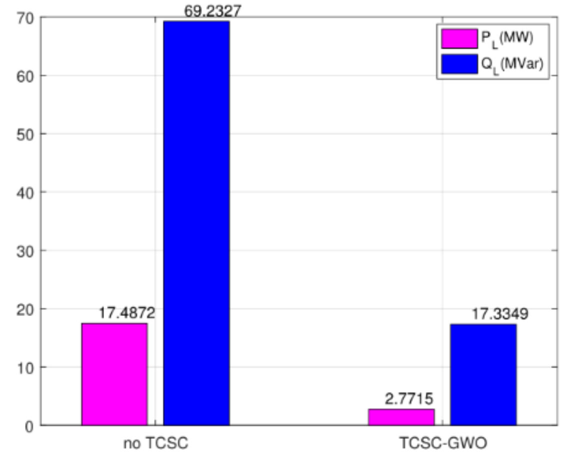

Fig:10 Active and Reactive power loss in Normal Loading using TCSC.

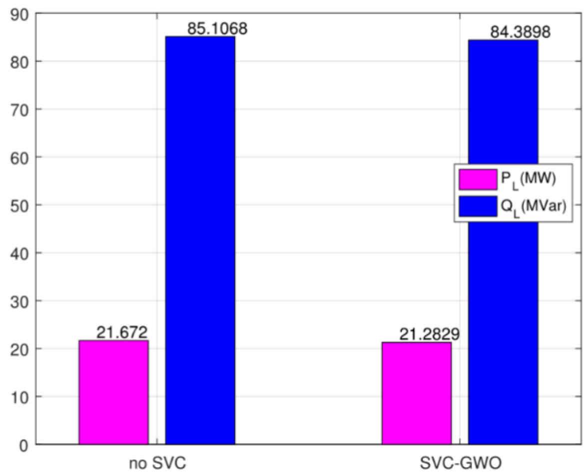

Fig:11 Active and Reactive power loss in 110% Over Loading using SVC

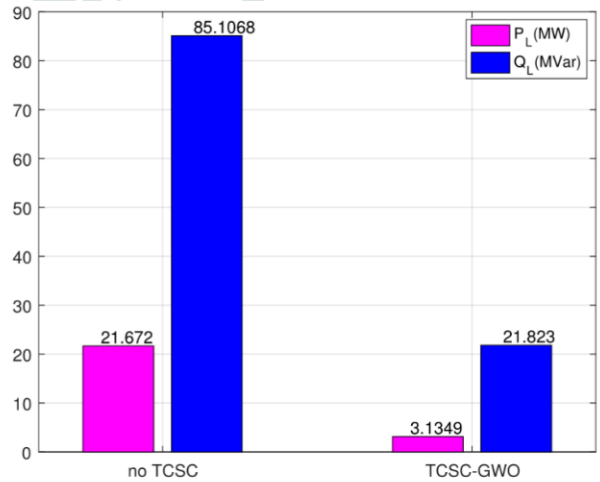

Fig :12 Active and Reactive power loss in 110% Over Loading using TCSC

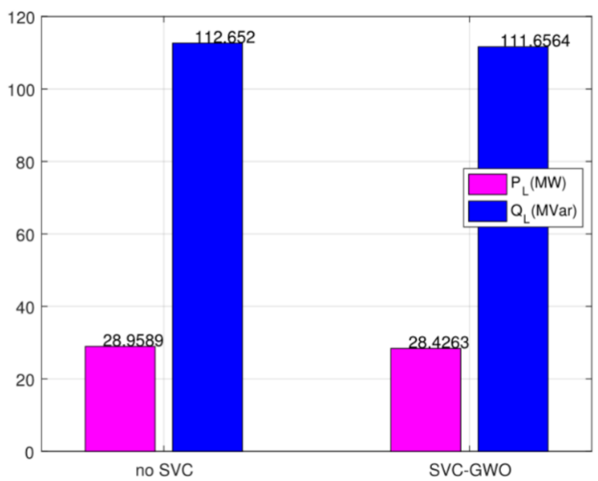

Fig:13 Active and Reactive power loss in 125% Over Loading using SVC

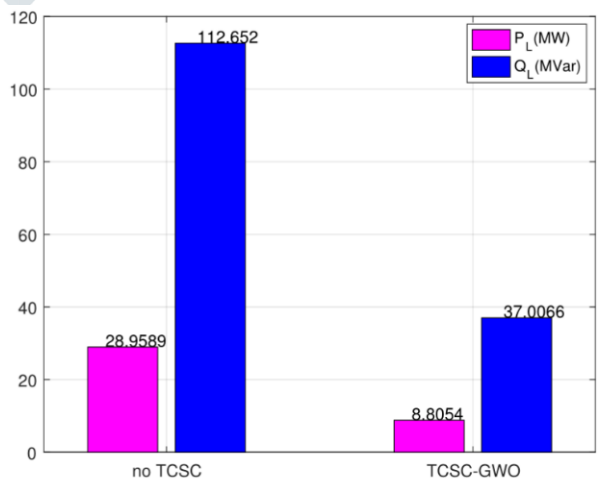

Fig :14 Active and Reactive power loss in 125% Over Loading using TCSC

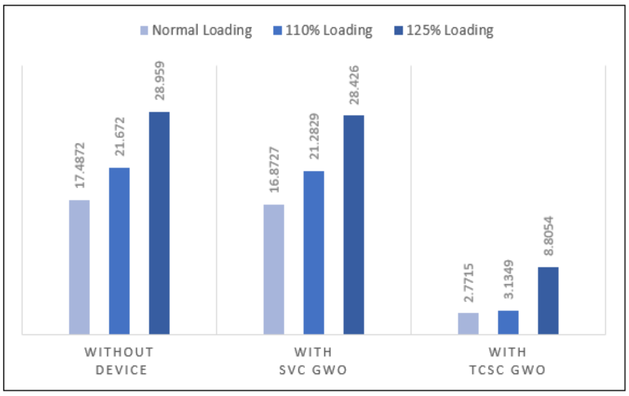

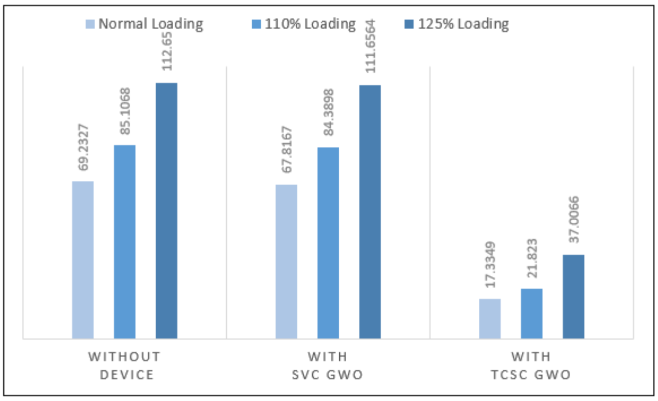

Fig 15: Comparison of Active power loss reduction by SVC and TCSC for different loading condition Fig 16: Comparison of Reactive power loss reduction bySVC and TCSC for different loading Conditions

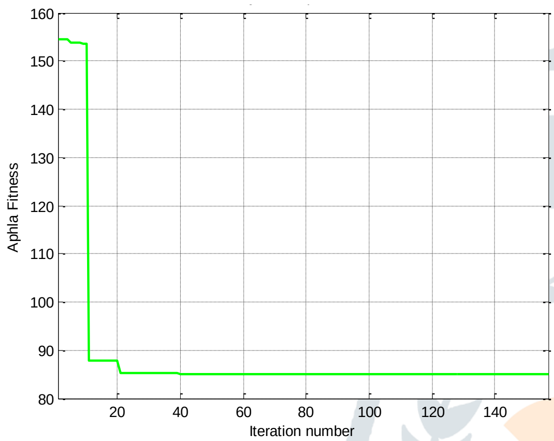

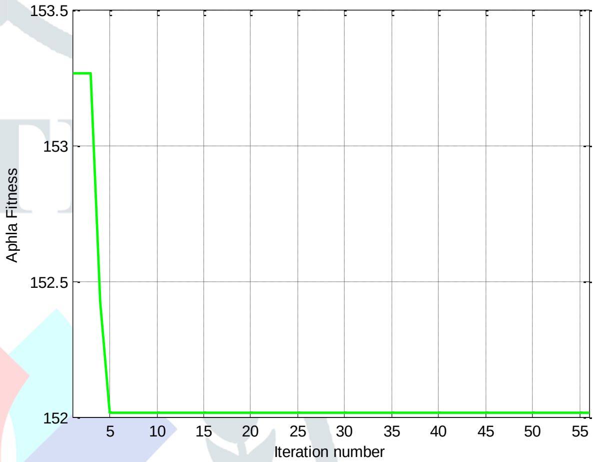

Fig17: GWO iteration graph (SVC-GWO) Fig 18: GWO iteration graph (TCSC-GWO)

Test Case 2, IEEE-57 Bus System:

Table no 3. Comparison of active & reactive power loss for different loading conditions using TCSC at different locations defined by GWO

Losses	Loading Condition	Without Device	With TCSC GWO	Location of TCSC (Line No.)	Xtcsc
Active Power Losses (MW)	Normal Loading	22.946	22.4652	18	0.2
	110% Loading	24.125	23.5646	12	0.2
	125% Loading	27.743	27.061	20	0.2
Reactive Power Losses (MVAR)	Normal Loading	112.71	112.5012	18	0.2
	110% Loading	115.38	115.2755	12	0.2
	125% Loading	128.77	128.0178	20	0.2

The same optimization technique was tested for IEEE 57 bus system also , which is again subjected to 110% and 125% overloading. As a result, the total active power demand raises to 880 MW (for 110% loading) and 1000 MW (for 125% loading) from normal loading requirement of 800 MW. After obtaining the optimal placement and sizing the TCSC reduces active power loss from 22.946 MW, 24.125MW & 27.743MW to 22.4652MW, 23.5646MW &27.061MW for normal, 110% overloading & 125% overloading respectively. Similarly TCSC minimized the reactive power from112.71 MVAR, 115.38MVAR &128.77MVAR to 112.5012MVAR, 115.2755MVAR &128.0178 MVAR for normal, 110% overloading & 125% overloading respectively.

Table no 3. Comparison of active & reactive power loss for different loading conditions using SVC at different locations defined by GWO

Losses	Loading Condition	Without Device	With SVC GWO	Location of SVC (Bus No.)	Bsvc
Active Power Losses (MW)	**Normal Loading**	22.946	22.8514	41	0.2500
	110% Loading	24.125	23.9646	16	0.2486
	125% Loading	27.743	27.4195	16	0.2477
Reactive Power Losses (MVAR)	**Normal Loading**	112.71	112.5221	41	0.2500
	110% Loading	115.38	115.4913	16	0.2486
	125% Loading	128.77	128.2866	16	0.2477

Optimal location of SVC is also obtained with GWO in IEEE 57 bus sytem and corresponding reduction of losses are shown table 3. Here again the active power loss is reduced from 22.946 MW, 24.125MW & 27.743MW to 22.8514MW, 23.9646MW &27.4195MW for normal, 110% overloading & 125% overloading respectively. Also reactive power losses minimized from 112.71 MVAR, 115.38 MVAR and 128.77MVAR to 112.5221 MVAR, 115.4913 MVAR and 128.2866 MVAR for normal ,110% and 125% overloading respectively.

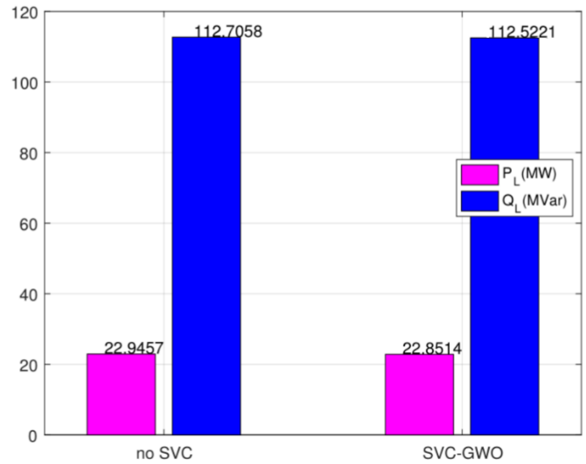

Fig:19 Active and Reactive power loss in Normal Loading using SVC

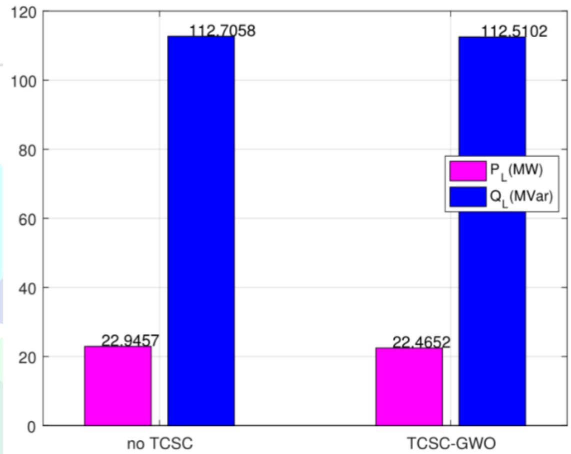

Fig:20 Active and Reactive power loss in Normal Loading using TCSC.

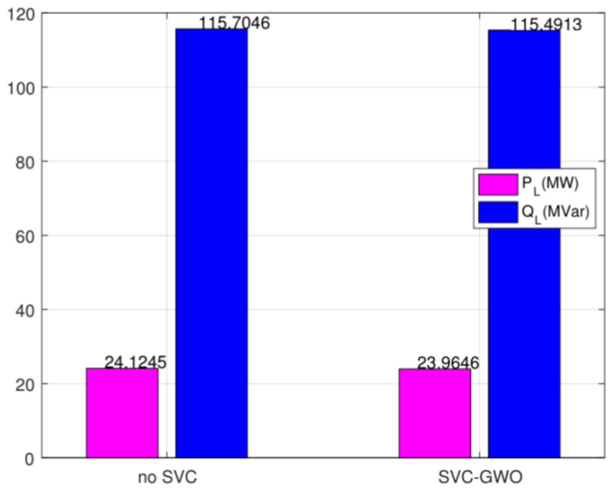

Fig:21 Active and Reactive power loss in 110% Over Loading using SVC

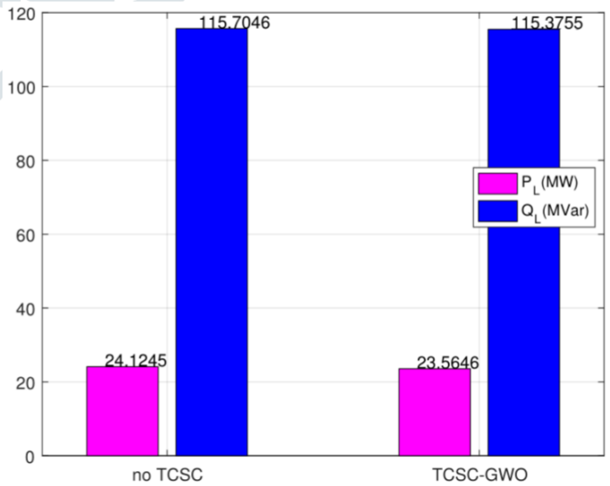

Fig :22 Active and Reactive power loss in 110% Over Loading using TCSC

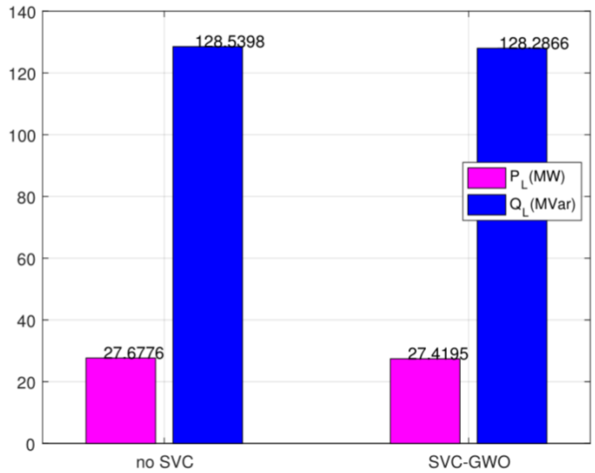

Fig:23 Active and Reactive power loss in 125% Over Loading using SVC

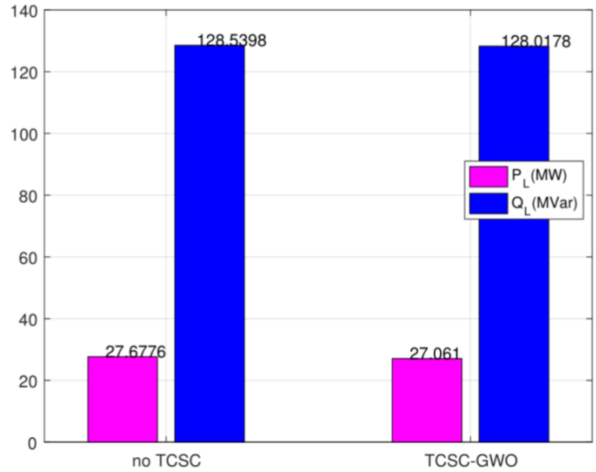

Fig :24 Active and Reactive power loss in 125% Over Loading using TCSC

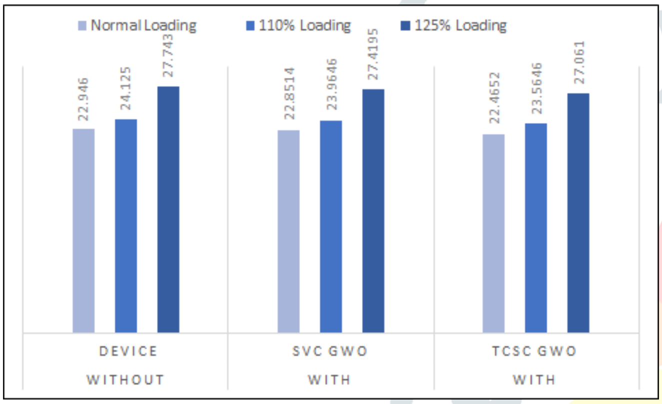

Fig 25: Comparison of Active power loss reduction by SVCand TCSC for different loading condition

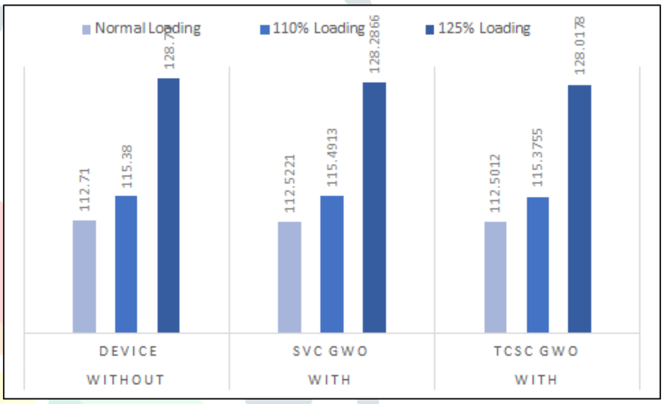

Fig 26: Comparison of Reactive power loss reduction by SVC and TCSC for different loading Conditions

Threrefore the GWO technique is an efficient method which considerably reduces the active and reactive power losses .Comparative study of the results of SVC and TCSC clearly depict that installation of TCSC effectively minimizes the system active and reactive power losses as compare to SVC.

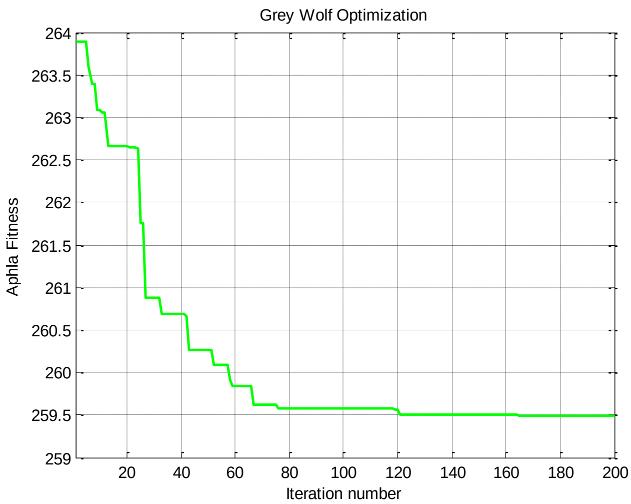

Fig 27: GWO iteration graph (SVC-GWO)

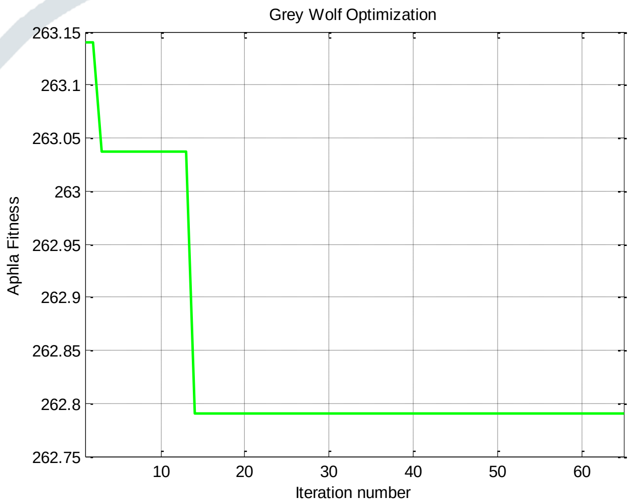

Fig 28: GWO iteration graph (TCSC-GWO)

X. CONCLUSION

This paper proposes a new solution technique for optimal placement of FACTS device, for active and reactive power loss reduction in IEEE 30 and IEEE 57 bus system under different loading conditions.In the latter and contrary to all the authors having treated this problem, we included in the objective function the reduction of the active &reactive losses of the power. Indeed, when capacitors are placed, the reactive components of the branch currents are reduced due to the prompt supply of reactive power and the active components of these currents also decrease due to the improvement of the voltage which results not only in reduction of the active power losses but also a reduction of the reactive power losses.

Furthermore the Newton-Raphson technique is used for load flow analysis. Grey Wolf Optimization is utilized for the optimization of sizing and location of FACT device (SVC and TCSC) for IEEE-30 and IEEE-57 bus test systems.From the results it is apparent that the proposed GWO based method reduces the power loss in both of the devices and TCSC is proved to be a better device to reduce the losses as compared to SVC.

REFERENCE

[1] Kaltenbach, J.C., Peschon, J. and Gehrig, E.H., 1970. A mathematical optimization technique for the expansion of electric power transmission systems. *IEEE Transactions on Power Apparatus and Systems*, (1), pp.113-119.
[2] Allaoua, B. and Laoufi, A., 2009. Optimal power flow solution using ant manners for electrical network. *Advances in Electrical and Computer Engineering*, *9*(1), pp.34-40.
[3] AlRashidi, M.R. and El-Hawary, M.E., 2009. A survey of particle swarm optimization applications in electric power systems. *IEEE transactions on evolutionary computation*, *13*(4), pp.913-918.
[4] Momoh, J.A., 2008. *Electric power system applications of optimization*. CRC press.
[5] Azim, S. and Swarup, K.S., 2005, December. Optimal capacitor allocation in radial distribution systems under APDRP. In *INDICON, 2005 Annual IEEE* (pp. 614-618). IEEE.
[6] Seifi, A. and Hesamzadeh, M.R., 2009. A hybrid optimization approach for distribution capacitor allocation considering varying load conditions. *International Journal of Electrical Power & Energy Systems*, *31*(10), pp.589-595.
[7] Guimaraes, M.A.N., Castro, C.A. and Romero, R., 2010. Distribution systems operation optimisation through reconfiguration and capacitor allocation by a dedicated genetic algorithm. *IET generation, transmission & distribution*, *4*(11), pp.1213-1222.
[8] Mekhamer, S.F., Soliman, S.A., Moustafa, M.A. and El-Hawary, M.E., 2003. Application of fuzzy logic for reactive-power compensation of radial distribution feeders. *IEEE transactions on power systems*, *18*(1), pp.206-213.
[9] Abdelaziz, A.Y., Mekhamer, S.F. and Nada, M.H., 2010. A fuzzy expert system for loss reduction and voltage control in radial distribution systems. *Electric Power Systems Research*, *80*(8), pp.893-897.
[10] Prakash, K. and Sydulu, M., 2007, June. Particle swarm optimization based capacitor placement on radial distribution systems. In *Power Engineering Society General Meeting, 2007. IEEE* (pp. 1-5). IEEE.
[11] Ziari, I., Ledwich, G., Ghosh, A., Cornforth, D. and Wishart, M., 2010. Optimal allocation and sizing of capacitors to minimize the transmission line loss and to improve the voltage profile. *Computers & Mathematics with Applications*, *60*(4), pp.1003-1013.
[12] Singh, S.P. and Rao, A.R., 2012. Optimal allocation of capacitors in distribution systems using particle swarm optimization. *International Journal of Electrical Power & Energy Systems*, *43*(1), pp.1267-1275.
[13] Hingorani, N.G., Gyugyi, L. and El-Hawary, M., 2000. *Understanding FACTS: concepts and technology of flexible AC transmission systems* (Vol. 2). New York: IEEE press.
[14] Shimpi, R.J., Desale, R.P., Patil, K.S., Rajput, J.L. and Chavan, S.B., 2010. Flexible AC transmission systems. *International Journal of Computer Applications*, *1*(15), pp.54-57.
[15] Luo, X., Wang, J., Dooner, M. and Clarke, J., 2015. Overview of current development in electrical energy storage technologies and the application potential in power system operation. *Applied Energy*, *137*, pp.511-536.
[16] El-Moursi, M.S. and Sharaf, A.M., 2006. Novel reactive power controllers for the STATCOM and SSSC. *Electric Power Systems Research*, *76*(4), pp.228-241.
[17] Kundur, P., Balu, N.J. and Lauby, M.G., 1994. *Power system stability and control* (Vol. 7). New York: McGraw-hill.
[18] Ibe, O.G. and Onyema, A.I., 2013. Concepts of reactive power control and voltage stability methods in power system network. *IOSR Journal of Computer Engineering*, *11*(2), pp.15-25.
[19] Singh, Y., 2013. Electrical resistivity measurements: a review. In *International journal of modern physics: Conference series* (Vol. 22, pp. 745-756). World Scientific Publishing Company.
[20] Yao, W., Jiang, L., Wen, J., Wu, Q. and Cheng, S., 2015. Wide-area damping controller for power system interarea oscillations: A networked predictive control approach. *IEEE Transactions on Control Systems Technology*, *23*(1), pp.27-36.
[21] Wang, Y., Yemula, P. and Bose, A., 2015. Decentralized communication and control systems for power system operation. *IEEE Transactions on Smart Grid*, *6*(2), pp.885-893.
[22] Abdullah, S.K.S., Sarmin, M.K., Saadun, N., Azmi, M.T., Abidin, I.Z. and Musirin, I., 2016. New generator and shunt reactive power control based secondary voltage control approach. *International Review of Automatic Control*, *9*(4), pp.192-206.
[23] Le, N.A.B.M., bin W Musa, W.M.N., binti Ismail, N., binti Ishak, N.H. and binti Salim, N.A., 2017. The Modeling of SVC for the Voltage Control in Power System. *Indonesian Journal of Electrical Engineering and Computer Science*, *6*(3).
[24] Romegialli, G. and Beeler, H., 1981, November. Reactive compensation. Problems and concepts of static compensator control. In *IEE Proceedings C (Generation, Transmission and Distribution)* (Vol. 128, No. 6, pp. 382-388). IET Digital Library.

[25] Taylor, C.W., Scott, G. and Hammad, A., 1994. Static var compensator models for power flow and dynamic performance simulation. *IEEE Transactions on Power Systems (Institute of Electrical and Electronics Engineers);(United States)*, *9*(1).

[26] Padiyar, K.R., 2008. *Power system dynamics*. BS publications.

[27] Erdman, W.L., US Windpower, Inc., 1993. *Static reactive power compensator*. U.S. Patent 5,187,427.

[28] Lee, S.Y., Wu, C.J. and Chang, W.N., 2001. A compact control algorithm for reactive power compensation and load balancing with static Var compensator. *Electric Power Systems Research*, *58*(2), pp.63-70.

[29] Ginarsa, I.M., Soeprijanto, A. and Purnomo, M.H., 2013. Controlling chaos and voltage collapse using an ANFIS-based composite controller-static var compensator in power systems. *International Journal of Electrical Power & Energy Systems*, *46*, pp.79-88.

[30] Lakdja, F. and Gherbi, F.Z., 2010. Impact of Thyristors Controlled Series Capacitor Devices and Optimal Power Flow on Power Systems. *Leonardo Journal of Sciences*, *9*(16), pp.145-157.

[31] Tabatabaei, N.M., Aghajani, G., Boushehri, N.S. and Shoarinejad, S., 2011. Optimal location of FACTS devices using adaptive particle swarm optimization mixed with simulated annealing. *International Journal on Technical and Physical Problems of Engineering (IJTPE)*, *7*, pp.60-70.

[32] Gitizadeh, M. and Kalantar, M., 2009. Optimum allocation of FACTS devices in Fars Regional Electric Network using genetic algorithm based goal attainment. *Journal of Zhejiang University-SCIENCE A*, *10*(4), pp.478-487.

[33] Ismail, M., Tawfik, G. and Hsen, H.A., 2012. Optimal location of multi type FACTS devices for multiple contingencies using genetic algorithms. *International Journal of Energy Engineering*, *2*(2), pp.29-35.

[34] Pali, B.S., Bhowmick, S. and Kumar, N., 2012, December. Newton-Raphson power flow models of static VAR compensator. In *Power Electronics (IICPE), 2012 IEEE 5th India International Conference on* (pp. 1-5). IEEE.

[35] Rathour, M.R.S. and Yadav, M.D.L., 2015. Newton Raphson TCSC Model for Power System Stability Improvement. *International Journal of Artificial Intelligence and Mechatronics*, *4*(2). pp. 35-40.

[36] Mirjalili, S., Mirjalili, S.M. and Lewis, A., 2014. Grey wolf optimizer. *Advances in Engineering Software*, *69*, pp.46-61.